Enhancing Antitumor Immune Responses by Optimized Combinations of Cell-penetrating Peptide-based Vaccines and Adjuvants

Elodie Belnoue[1], Wilma Di Berardino-Besson[2], Hubert Gaertner[3], Susanna Carboni[1], Isabelle Dunand-Sauthier[3], Fabrice Cerini[3], Else-Marit Suso-Inderberg[4], Sébastien Wälchli[4,5], Stéphane König[6], Andres M Salazar[7], Oliver Hartley[3], Pierre-Yves Dietrich[2], Paul R Walker[2] and Madiha Derouazi[1]

[1]Amal Therapeutics, Geneva, Switzerland; [2]Center of Oncology, Geneva University Hospitals and University of Geneva, Geneva, Switzerland; [3]Department of Pathology and Immunology, University of Geneva, Geneva, Switzerland; [4]Department of Cellular Therapy, Oslo University Hospital Radiumhospitalet, Oslo, Norway; [5]Department of Cancer Immunology, Institute for Cancer Research, Oslo University Hospital Radiumhospitalet, Oslo, Norway; [6]Department of Basic Neurosciences, University of Geneva, Geneva, Switzerland; [7]Oncovir, Washington DC, USA

Cell penetrating peptides (CPPs) from the protein ZEBRA are promising candidates to exploit in therapeutic cancer vaccines, since they can transport antigenic cargos into dendritic cells and induce tumor-specific T cells. Employing CPPs for a given cancer indication will require engineering to include relevant tumor-associated epitopes, administration with an appropriate adjuvant, and testing for antitumor immunity. We assessed the importance of structural characteristics, efficiency of *in vitro* transduction of target cells, and choice of adjuvant in inducing the two key elements in antitumor immunity, CD4 and CD8 T cells, as well as control of tumor growth *in vivo*. Structural characteristics associated with CPP function varied according to CPP truncations and cargo epitope composition, and correlated with *in vitro* transduction efficiency. However, subsequent *in vivo* capacity to induce CD4 and CD8 T cells was not always predicted by *in vitro* results. We determined that the critical parameter for *in vivo* efficacy using aggressive mouse tumor models was the choice of adjuvant. Optimal pairing of a particular ZEBRA-CPP sequence and antigenic cargo together with adjuvant induced potent antitumor immunity. Our results highlight the irreplaceable role of *in vivo* testing of novel vaccine constructs together with adjuvants to select combinations for further development.

Received 29 February 2016; accepted 17 June 2016; advance online publication 9 August 2016. doi:10.1038/mt.2016.134

INTRODUCTION

The therapeutic potential of tumor-specific immune responses is well recognized and is critical for cancer vaccine development. Nevertheless, such development is a complex task that integrates many components.[1] Indeed, solid tumors are composed of heterogeneous cancer cells expressing diverse antigens, with immunosuppressive microenvironments; accessibility for immune effector cells and molecules is variable.[2–4] Although the immune system can recognize and, to some extent, eliminate tumor cells, the antitumor immune response often remains of low amplitude and is inefficient.[5] Boosting antitumor immunity with therapeutic vaccination is a long sought goal of cancer therapy. However, the identification of optimal combinations of antigens, adjuvants, and delivery processes has not yet been achieved.[6]

Several novel ideas about how to manipulate parameters to facilitate the development of more potent cancer vaccines are emerging. Cancer vaccines must deliver antigens to antigen-presenting cells such as dendritic cells (DCs) and activate them. In addition, cancer vaccines should stimulate both CD4 T helper cells and CD8 cytotoxic T cells specific for different epitopes. Protein vaccines allow multiepitopic antigen delivery to DCs with long-lasting epitope presentation.[7] They also require uptake and processing by DCs to achieve major histocompatibility complex (MHC)-restricted presentation of their constituent epitopes. Overall, these mechanisms reduce the risk of peripheral tolerance that was described after vaccination with short peptides.[8] However, most soluble proteins are generally degraded in endolysosomes and are poorly cross-presented on MHC class I molecules, inducing no or low-level CD8 T cell responses.[9] We have previously demonstrated that the efficacy of protein-based vaccine delivery could be improved by the use of cell penetrating peptides (CPPs).[10]

CPPs are peptides of 8–40 residues that have the ability to cross the cell membrane and enter into most cell types.[11,12] The best described is the trans-activating transcriptional activator from the human immunodeficiency virus 1 (HIV-TAT),[13,14] but CPPs of different origins are now known.[15,16] The secondary structure of CPPs is an important feature for their cellular uptake,[17] with helical structure being associated with strong CPP-membrane interactions.[18] Recently, a CPP derived from the viral protein ZEBRA was described to transduce protein cargoes across membranes by both direct translocation and lipid raft-mediated endocytosis.[19]

Correspondence: Madiha Derouazi, Amal Therapeutics, c/o Fondation pour Recherches Médicales. 64 av. de la Roseraie, 1205 Geneva, Switzerland. *E-mail:* madiha.derouazi@amaltherapeutics.com

We previously showed that these two mechanisms of entry promote both MHC class I and II restricted presentation of cargo antigens to CD8 and CD4 T cells, respectively. We demonstrated that a fusion protein combining ZEBRA CPP with a multiantigenic protein was able to deliver multiepitope peptides to DCs, and subsequently to promote cytotoxic T lymphocyte (CTL) and Th cell activation, and antitumor function.[10]

Here, we have identified truncations of ZEBRA CPP with different structural characteristics that markedly improve antigen-specific CD8 and CD4 T cell immune responses both *in vitro* and *in vivo*. Responses were assessed not only to the model antigen ovalbumin (OVA), but also to the human melanoma/melanocyte proteins gp100 and MART-1, and to tyrosinase related protein 2(Trp2). Vaccination experiments using different adjuvants were performed in both naive and tumor-bearing mice and optimal ZEBRA CPP-adjuvant combinations impacting on both subcutaneous (s.c.) tumors and lung metastases were characterized. Collectively, these data enhance our understanding of CPP-adjuvant combinations that can be further developed for optimal clinical efficacy.

RESULTS

Circular dichroism analysis of ZEBRA CPP variants

Eight variants of ZEBRA CPP were designed (see **Supplementary Figure S1**) based on Z12 full-length CPP sequence.[10] To avoid the disulfide bridges during protein production and purification processes, the cysteine residue in Z12 was replaced by a serine residue in the variant Z13. Based on their theoretical isoelectric point (pI) and secondary structure, truncations were then designed from Z13 variant sequence. Due to their amino acid sequence and their size, the variants had different physicochemical properties (see **Supplementary Table S1**). The N-terminal truncated CPPs (Z13–Z15 and Z19–Z20) were more hydrophobic, whereas the C-ter truncated CPPs (Z16–Z18) were highly positively charged. With its very low pI, Z16 CPP truncation was not expected to be a highly potent CPP.[20] New vaccine constructs were designed by conjugating each of the eight ZEBRA CPP variants to the highly hydrophobic MHC class-I restricted epitope from model antigen OVA (OVACD8). The conjugation with the OVACD8 epitope resulted in a isoelectric point (pI) decrease and in an increase of hydrophobicity (see **Supplementary Table S2**). These variants were first studied by circular dichroism analysis which represents the technique of choice to estimate secondary structures of proteins and peptides in solution.[21] Alpha-helical structures, reported to control to a certain extent their cellular uptake,[18] are usually characterized by the presence of two negative bands at 208 and 222 nm along with one positive band at 192 nm. Circular dichroism analysis showed that almost all CPP constructs assessed exhibited an alpha-helical conformation but this secondary structure seemed to be favored in some of the shortest constructs Z15-, Z16-, and Z20-conjugates (**Figure 1**). These results pointed out that the conjugated epitope could significantly contribute to the overall helical content of the construct, which could potentially influence the CPP properties.

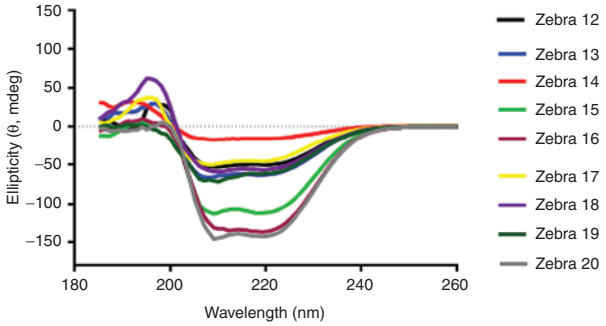

Figure 1 CD spectroscopy of Z12–Z20 variant conjugated to OVACD8 epitope. All peptides were measured at 100 µmol/l concentration in water containing 1.25% trifluoroethanol.

Capacity of ZEBRA CPP variants to promote cross-presentation

The functionality of the different ZEBRA CPP variants was validated both *in vitro* and *in vivo*, based on the capacity to stimulate OVA-specific CD8 T cells (from OT-I T cell receptor (TCR) transgenic mice). This capacity should reflect transport of the OVACD8 cargo into antigen-presenting cells. The read-out for these experiments was the proliferation of OVA-specific CD8 T cells *in vitro* (**Figure 2a**), and for the *in vivo* studies, the induction of OVA-specific CD8 T cells in the blood of mice vaccinated with the different CPP-OVACD8 conjugates together with adjuvant (**Figure 2b**). CPPs variants generally conserved their immunogenicity, but the *in vitro* tests showed little discrimination between them. In contrast, the *in vivo* vaccination experiments showed more pronounced differences: Z13, Z14, Z15, and Z18 elicited significant higher frequencies of antigen specific CD8 T cells compared with adjuvant control. Thus, we selected these variants for further studies with full-length Z13 as a reference.

In vitro transduction with the ZEBRA CPP variants

In order to assess more directly, the transduction capacities of the selected CPP variants, fluorescent constructs were tested using different cell types. Most importantly, we tested DCs of both human and mouse origin as the phagocytic antigen-presenting cell most critical for antigen presentation. In addition, we included two cell lines: murine EL4 thymoma cells and human K562 erythroleukemia line (**Figure 3**). Transduction efficacy was different depending on the cell type for truncated Z14 and Z15, while full-length Z13 was of comparable efficiency on all investigated cell lines. All the peptides showed a modest transduction using DCs of murine origin. The variant Z18 with the lowest pI exhibited a lower transduction efficiency compared with other CPP variants, for all cell lines tested. This was in accordance with a positive correlation between the transduction efficacy and the theoretical pI value (see **Supplementary Figure S2a**). Overall, transduction efficiency was greater for human DCs, which might be correlated to phagocytic activity, showing that results are translatable to human cells.

In vitro capacity of ZEBRA CPP variants to promote epitope presentation on MHC class I and MHC class II

We extended our studies using Z13, Z14, Z15, and Z18 CPPs to transduce human DCs with the human leukocyte antigen (HLA)-A2 epitope of the tumor associated antigen (TAA) MART1 as cargo. The physicochemical properties of these new construct show that conjugation with the MART1 epitope resulted

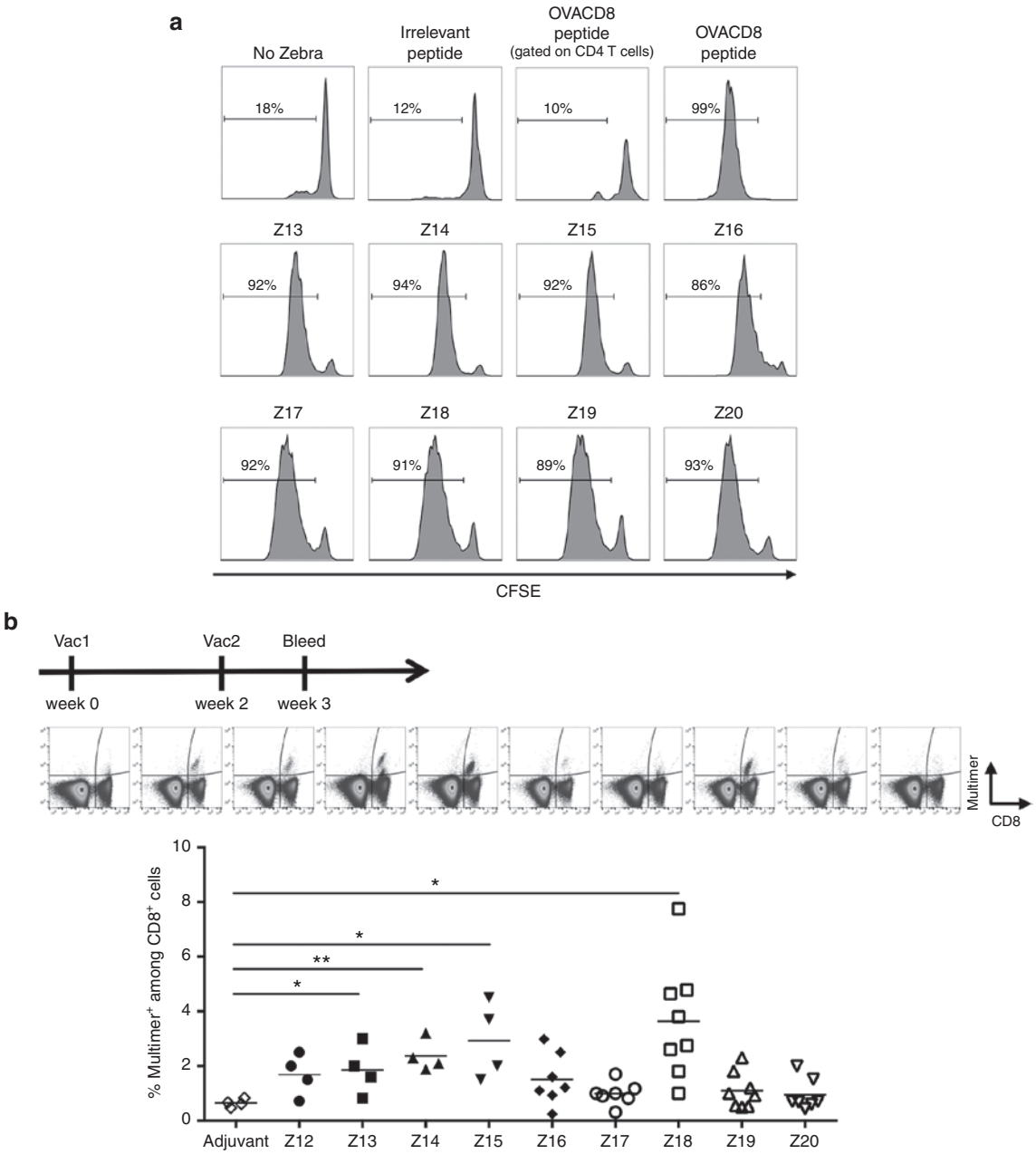

Figure 2 Identification of the most potent CPP truncations *in vitro* (proliferation assay) and *in vivo* (CD8 T cell immune response after vaccination). (**a**) Processing of each ZEBRA CPP truncation (conjugated to OVACD8 epitope) by BMDCs and antigen presentation to $OVA_{257–264}$ specific, MHC class I restricted (H-$2K^b$) OT-I T cells *in vitro*. CFSE-labeled splenocytes from OT-I mice were cocultured for 4 days alone, or with mature BMDCs that had been loaded with each ZEBRA CPP truncation (Z13– Z20). Negative controls include OT1 incubated with non-loaded BMDCs or BMDCs loaded with irrelevant peptide (gp100 peptide). A positive control was performed by stimulating OT1 cells with BMDCs loaded with OVACD8 peptide. Except when indicated, proliferation was assessed by CFSE dilution analyzed by flow cytometry, gating on live CD8 T cells. Data from one experiment representative of two independent experiments. (**b**) C57BL/6 mice were vaccinated by s.c. injection at wk0, and wk2 with 10 nmoles of each ZEBRA CPP truncation (Z12–Z20) conjugated to OVACD8 epitope and mixed with 100 µg of anti-CD40. Mice were also injected with 50 µg of Hiltonol i.m. (same side as the s.c. injection). Adjuvant control mice received anti-CD40 and Hiltonol. Mice were bled 1 week after the second vaccination for assessing OVA-specific CD8 T cells. Data from two independent experiments are shown. One representative dot-plot of each group is shown. $*P < 0.05$; $**P < 0.01$ (Kruskal–Wallis test). BMDC, bone marrow derived DCs; CPP, cell penetrating peptide; CFSE, carboxyfluorescein diacetate succinimidyl ester; OVA, ovalbumin.

in a decrease of the pI and a strong hydrophobicity increase (see **Supplementary Table S3**). As shown, efficient stimulation of human MART1-specific CD8 T cells was CPP dependent as no response was detected with scramble construct (**Figure 4**). We also observed similar cytokine expression and degranulation marker CD107a expression for Z13, Z14, and Z15 CPPs. Again, only Z18 CPP, the variant with the lowest pI showed markedly lower efficacy. Interestingly, the epitope presentation capacity was significantly correlated to the pI value (see **Supplementary Figure S2b**).

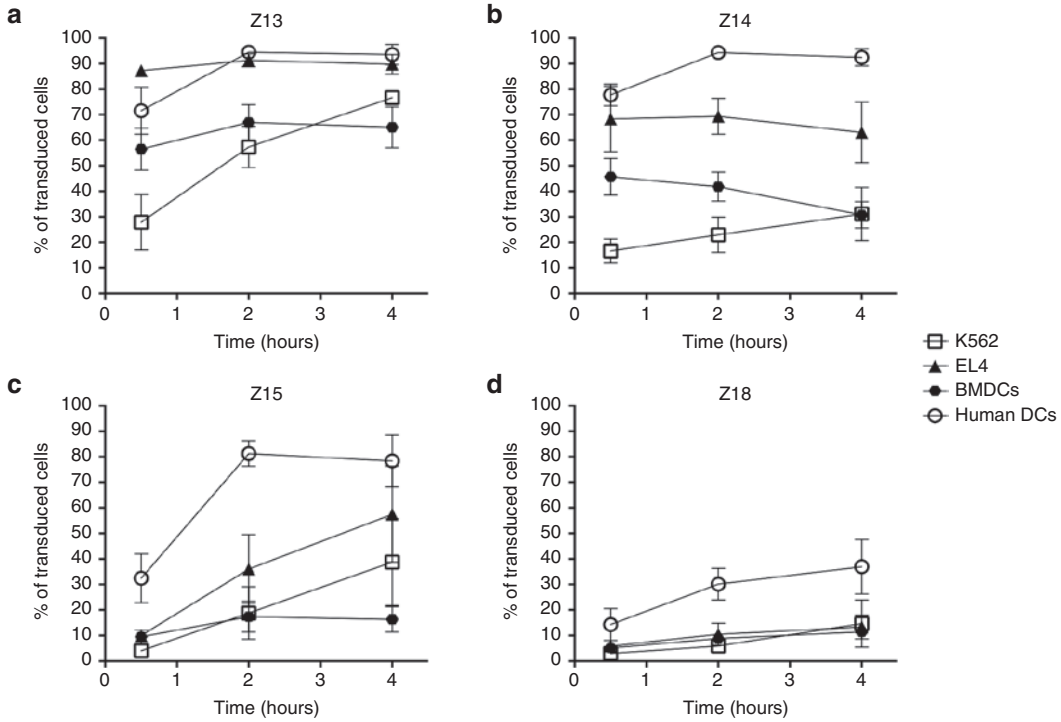

Figure 3 Comparison of the transduction capacity of Z13, Z14, Z15, and Z18 CPP truncations. Transduction was assessed in cells with high phagocytosis capacity (DCs of human and mice origin) and in cells with poor phagocytosis capacity (human K562, or murine EL4). Cells were incubated for 30 minutes, 2 hours or 4 hours with the fluorescein-conjugated constructs (Z13OVACD8FAM, Z14OVACD8FAM, Z15OVACD8FAM or Z18OVACD8FAM) then subjected to a 30 seconds wash with an acidic buffer to remove membrane bound peptide before staining for flow cytometry analysis. Mean and SEM of three independent experiments are shown. DC, dendritic cells; CPP, cell penetrating peptide; OVA, ovalbumin.

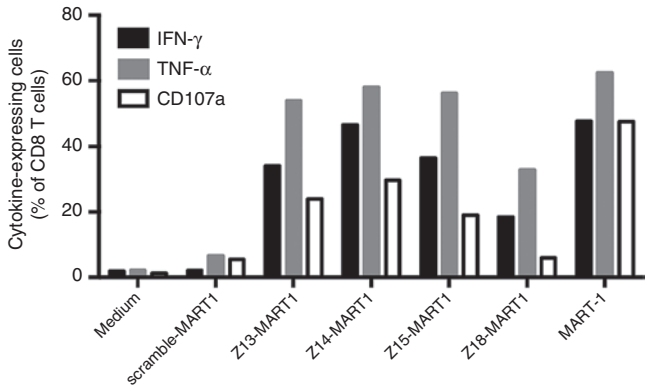

Figure 4 *In vitro* epitope presentation (MHC I-restricted) assay by human DCs. Human monocyte-derived DCs were loaded with 1 µmol/l of scramble-MART1, Z13-MART1, Z14-MART1, Z15-MART1 or Z18-MART1 for 4 hours, washed and then incubated overnight at 37°C. In addition nonloaded DCs and DCs loaded with the high affinity peptide MART-1 were used as negative and positive controls, respectively. Specific TCR-transfected T cells were then added to DCs and incubated for 5 hours with monensin and brefeldinA before staining for flow cytometry. Data from one experiment representative of two independent experiments. DCs, dendritic cells; CPP, cell penetrating peptide; TCR, T cell receptor; MHC, major histocompatibility complex.

Next, we tested the capacity of the CPP variants to stimulate not only CD8 cytotoxic T cells, but also CD4 helper T cells. This mechanism is essential for robust integrated antitumor immune responses. For this purpose, antigenic cargos including both CD8 and CD4 T cell epitopes from OVA were conjugated to Z13, Z14, Z15, and Z18. The addition of OVACD4 epitope caused a pI decrease and a hydrophobicity increase (see **Supplementary Table S4**). With its low pI, Z18 construct is not expected to be strongly efficacious. Processing and presentation of the CD8 and CD4 T cell epitopes were monitored by measuring the *in vitro* proliferation of naive OVA-specific T cells from OT-I and OT-II TCR transgenic mice, respectively (**Figure 5**). Proliferation of both CD8 and CD4 T cells occurred *in vitro* with all ZEBRA CPP variants, confirming an efficient transduction of the DCs and delivery of the cargo into antigen processing pathways for both MHC class I and MHC class II. However, for both pathways, Z18 was less efficient than Z13, Z14 or Z15, suggesting again that physicochemical properties of ZEBRA CPP variants were quite predictive of *in vitro* results.

Taken together, the results confirmed that all tested CPP variants were able to deliver their antigenic cargo into the different processing compartments of DCs, with results of truncated Z14 and Z15 being comparable with full-length Z13, while Z18 being more modest.

Capacity of ZEBRA CPP variants vaccines to elicit OVA-specific CD8 and CD4 T cell immune responses by combination with different adjuvants

To extend the previous findings to *in vivo* vaccination, Z13, Z14, Z15, and Z18 conjugated to antigenic cargo containing both OVACD8 and OVACD4 epitopes were first tested with Hiltonol adjuvant (a Toll-like receptor-3 (TLR3) agonist). Agonistic antibody to CD40, which could substitute for CD4

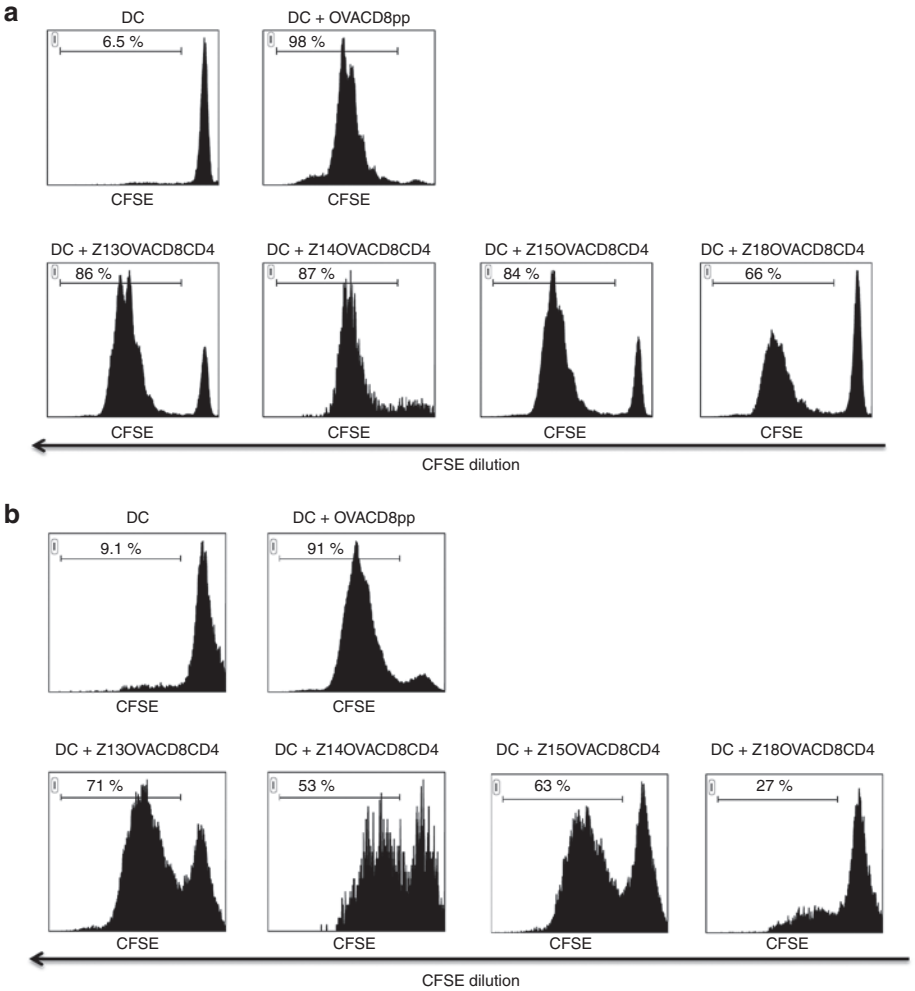

Figure 5 ***In vitro*** **epitope presentation (MHC I and MHC II-restricted) assay.** Processing of Z13OVACD8CD4, Z14OVACD8CD4, Z15OVACD8CD4, and Z18OVACD8CD4 by BMDCs and antigen presentation to $OVA_{257–264}$ specific, MHC class I restricted (H-2K^b) OT-I T cells (**a**) or to $OVA_{323-339}$ specific, MHC class II restricted (H-2IA^b) OT-II T cells (**b**) *in vitro*. CFSE-labeled splenocytes from OT-I or OT-II mice were cocultured for 4 days alone with mature BMDCs that had been loaded with each ZEBRA CPP construct. Proliferation was assessed by CFSE dilution analyzed by flow cytometry, gating on live CD8 (OT-I cells, **a**) or CD4 (OT-II cells, **b**) T cells. As positive control, BMDCs were pulsed for 1 hour with 5 µmol/l peptide. Data from one experiment representative of three independent experiments. BMDC, bone marrow derived DCs; CPP, cell penetrating peptide; MHC, ; CFSE, carboxyfluorescein diacetate succinimidyl ester; OVA, ovalbumin.

T cell help,[22] was not added in these following series of experiments, given the presence of the CD4 epitope in the constructs. A control construct without ZEBRA CPP was also assessed. OVA-specific CD4 and CD8 T cells were evaluated by quantifying interferon-γ (IFN- γ) secreting cells (**Figure 6a**,**b**). Alone, the cargo elicited low CD4 and CD8 T cell immune responses. In contrast, CD8 T cell responses were enhanced in mice vaccinated with constructs conjugated to Z13, Z14 or Z18 CPP (**Figure 6a**), proving the critical role of ZEBRA CPP. This was confirmed by MHC-peptide multimer staining for Z13 and Z18 CPP (see **Supplementary Figure S3a**) and intracellular staining (see **Supplementary Figure S3b**). The highest CD4 T cell responses were observed when mice were vaccinated with Z15 or Z18 CPP constructs as shown by the quantification of IFN-γ-producing OVA-specific CD4 T cells (**Figure 6b**), confirmed also by the proportion of multifunctional CD4 T cells producing IFN-γ, interleukin(IL)2 and tumor necrosis factor (TNF)-α (see **Supplementary Figure S2c**).

In parallel, we evaluated the T cell immune responses elicited by vaccination with the same constructs and the TLR2 adjuvant Pam3CSK4. Strikingly, mixed with this adjuvant, the Z18 CPP construct induced the highest number of specific CD8 T cell responses (**Figure 6c** and **Supplementary Figure S4a**). In addition, this construct was the most efficacious at eliciting CD4 T cell immune responses (**Figure 6d**).

As the combination of the adjuvant with the ZEBRA CPP construct seemed to be critical for eliciting potent immune responses *in vivo*, a third adjuvant, the TLR4 adjuvant MPLA with Monophosphoryl Lipid A (MPLA) was tested combined with the different CPP constructs. Combined with MPLA, the Z13 CPP construct elicited higher CD8 and CD4 T cell responses compared to shorter constructs (**Figure 6e**,**f** and **Supplementary Figure S4b**).

Taken together, the data showed that the combination of the ZEBRA CPP variant and the adjuvant is an important issue. As an *e.g.*, Z18 induced the highest CD8 and CD4 immune response

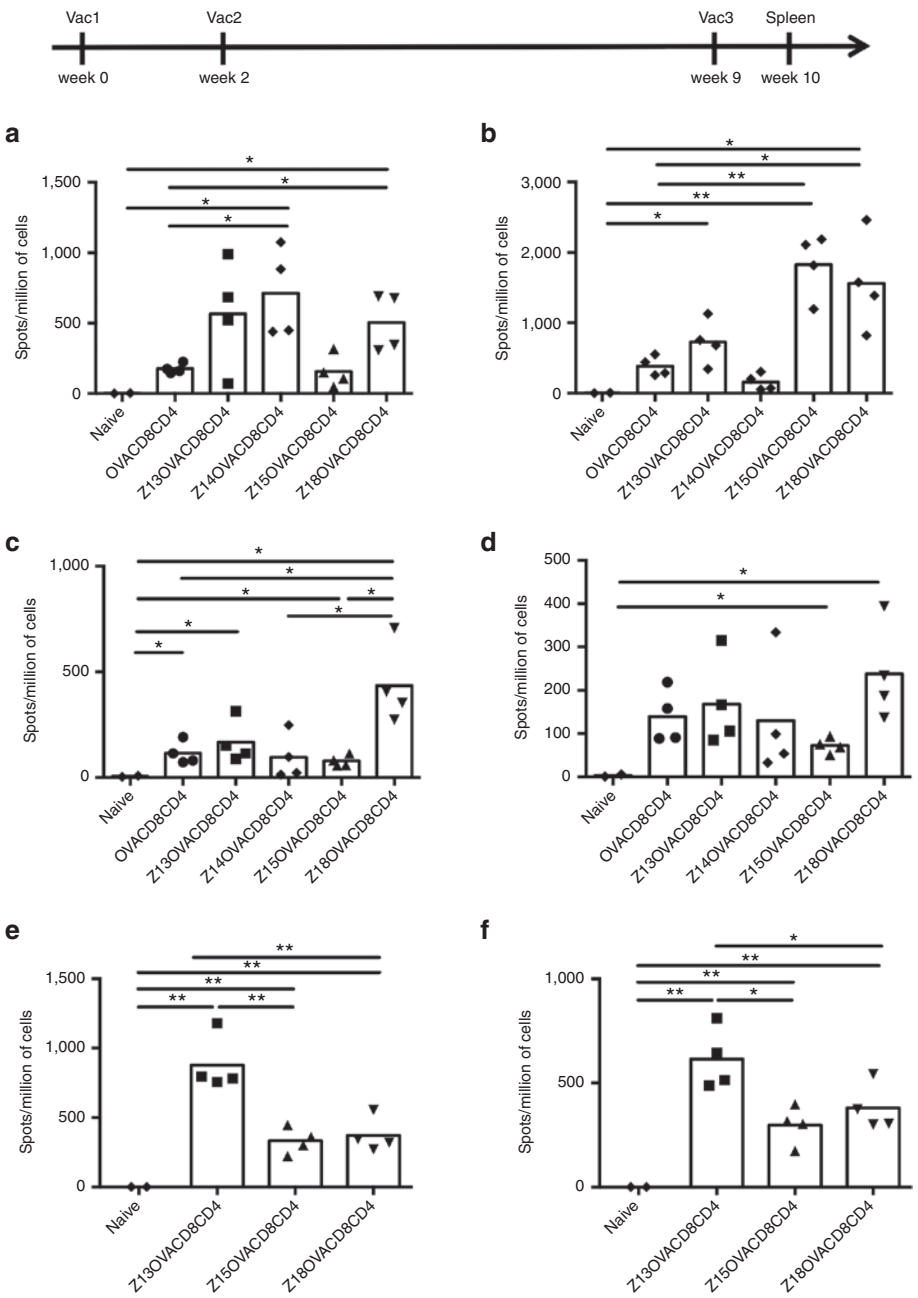

Figure 6 CD8 and CD4 T cell immune responses elicited by vaccination with CPP truncations combined to different adjuvants. Mice were vaccinated three times (wk0, wk2, and wk9) by s.c. injection of 10 nmoles of OVACD8CD4 (the cargo without ZEBRA CPP), Z13OVACD8CD4, Z14OVACD8CD4, Z15OVACD8CD4, Z18OVACD8CD4, and i.m. injection of 50 µg of Hiltonol (**a** and **b**), or mixed with 20 µg of Pam3CSK4 (**c** and **d**) or with 20 µg of MPLA. After 1 week from last vaccination, ELISPOT assay was performed on spleen cells for detecting IFN-γ-producing $OVA_{257-264}$-specific CD8 T cells (**a**, **c**, and **e**) and $OVA_{323-339}$–specific CD4 T cells (**b**, **d,** and **f**). Data from one experiment representative of two independent experiments. *$P < 0.05$; **$P < 0.01$. CPP, cell penetrating peptide; MPLA, Monophosphoryl Lipid A; IFN, interferon; ELISPOT, enzyme-linked immunospot; OVA, ovalbumin.

when combined with Pam3CSK4, whereas Z13 was more efficacious when combined with MPLA. However, MPLA and Pam3CSK4 elicited CD4 T cell immune responses at a lower level compared to Hiltonol, reported to be a highly potent adjuvant for T helper responses.[23,24] Even the Z15 CPP, which elicited lower T cell immune responses with any adjuvant, was capable of promoting high CD4 T cell responses when combined with Hiltonol.

Therapeutic effect of ZEBRA CPP variant vaccines to control tumor growth

Next, we evaluated the therapeutic effect (on tumor growth) of T cell immune responses elicited by the different combinations of ZEBRA CPP constructs with the different adjuvants. For this purpose, mice were implanted s.c. with 3×10^5 EG7-OVA cells in the left flank and vaccinated in the right flank 3 times in a therapeutic setting; 5, 13, and 21 days post-tumor implantation (**Figure 7**).

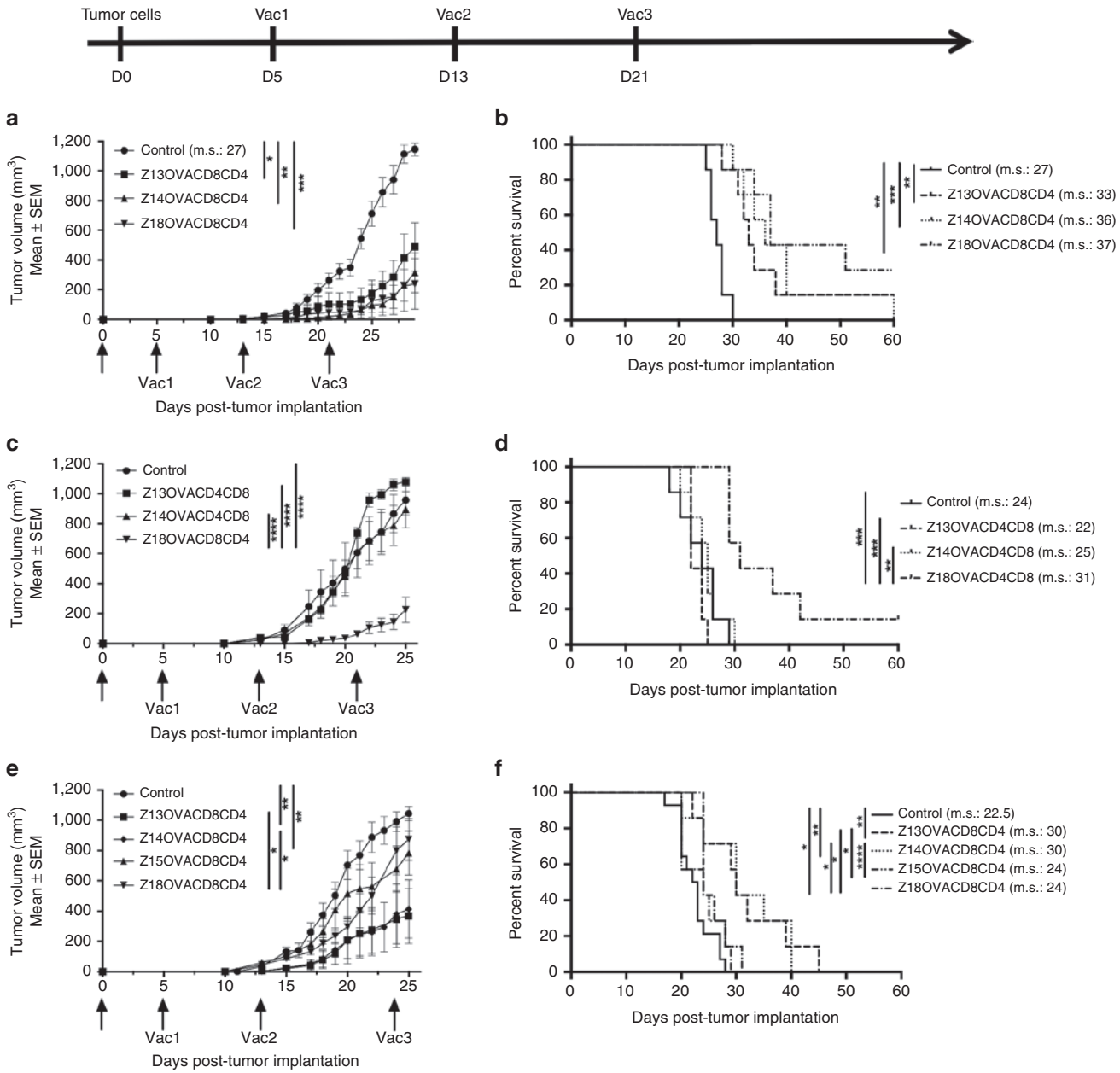

Figure 7 Therapeutic effect of CPP truncations on tumor growth. C57BL/6 mice were implanted s.c. with 3×10^5 EG7-OVA tumor cells in the left flank and vaccinated three times (d5, d13, and d21) by s.c. injection of 10 nmoles of Z-truncOVACD8CD4 peptides and 50 µg of Hiltonol (**a**,**b**) or 20 µg of Pam3CSK4 (**c**,**d**) or 20 µg of MPLA (**e**,**f**) in the right flank. Tumor size was measured with a caliper. **a**, **c** and **e**: tumor growth (mean of 7 mice per group ± SEM). *$P < 0.05$; **$P < 0.01$; ***$P < 0.001$; ****$P < 0.0001$ (two-way analysis of variance test at the day when tumor size of all control mice reach a size superior to 1,000 mm^3). **b**, **d**, and **f**: survival curve of 7 mice per group. Median survival is indicated on the graph (m.s.). *$P < 0.05$; **$P < 0.01$; ***$P < 0.001$; ****$P < 0.0001$ (Log-Rank test). CPP, cell penetrating peptide; MPLA, Monophosphoryl Lipid A; OVA, ovalbumin.

With Hiltonol, each ZEBRA CPP construct was able to significantly delay tumor growth. In contrast, only Z18 was efficacious to control tumor growth when the ZEBRA CPP construct was injected with Pam3CSK4 adjuvant. This was not the case when ZEBRA CPP constructs were used in combination with MPLA: in this case, Z13 and Z14 CPP were the most efficacious. These results confirm previous immune response data (**Figure 6**) and point out the importance of the adjuvant combination for the overall therapeutic response.

Capacity of ZEBRA CPP variants vaccines to elicit gp100-specific CD8 T cell immune responses

To extend the previous results, OVACD8 epitope was replaced by the TAA $gp100_{25–33}$ CD8 epitope in the previous constructs (see **Supplementary Table S5**) to evaluate the TAA-specific immune response. These constructs were tested with Hiltonol (**Figure 8a**) or MPLA adjuvant (**Figure 8b**). Although OVA-specific CD4 T cells were elicited in all groups (not shown), the data indicated that Z18 elicited poor gp100-specific CD8 T cell responses. In

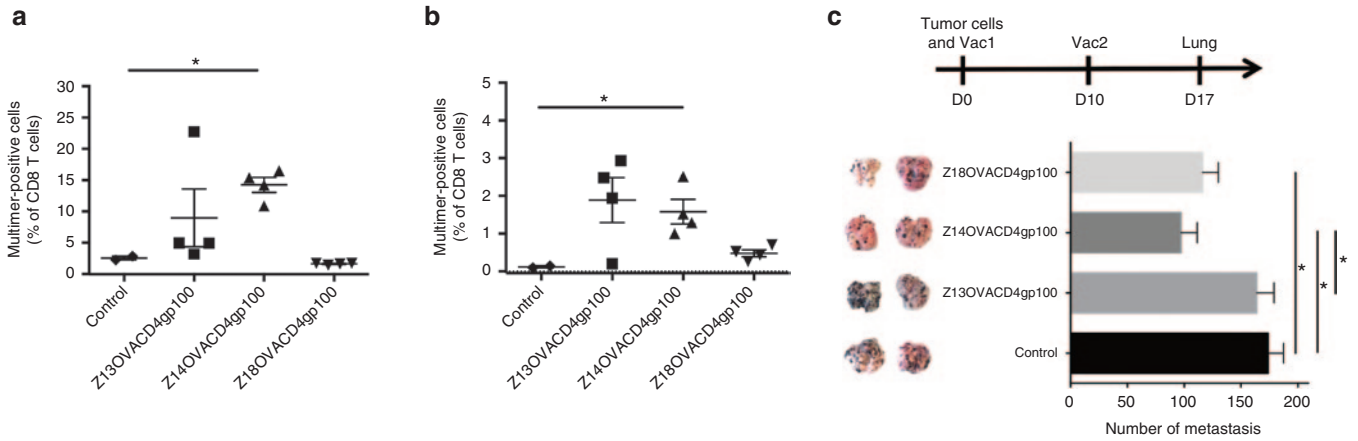

Figure 8 TAA-specific CD8 T cell immune responses elicited by vaccination with CPP truncations and effect of CPP truncations on control of melanoma lung metastasis growth. (**a**, **b**) Mice were vaccinated three times (wk0, wk2, and wk5) by s.c. injection (right flank) of 10 nmoles of Z13OVACD4gp100CD8, Z14OVACD4gp100CD8, Z18OVACD4gp100CD8 and i.m. injection of 50 µg of Hiltonol (right hind leg) (**a**) or four times (wk0, wk2, wk4, and wk7) by s.c. injection (right flank) of 10 nmoles of same constructs mixed with 20 µg of MPLA (**b**). After 1 week from the last vaccination, spleen cells were restimulated *in vitro* for 7 days with $gp100_{25-33}$ peptide and multimer staining was performed. (**c**) Mice were vaccinated twice (d-21 and d-7) by s.c. injection of 2 nmoles of Z13OVACD4gp100, Z14OVACD4gp100 or Z18OVACD4gp100 mixed with 100 µg of anti-CD40 and by i.m. injection of 50 µg of Hiltonol (right hind leg) and implanted i.v. with 1×10^5 B16-OVA melanoma tumor cells at day 0. Mice were euthanized at day 17 and lung recovered. Control mice group was injected with anti-CD40 and Hiltonol only. Number of metastasis foci was counted for each lung (5–7 mice/group). Two representative lung pictures of each group are shown. $^*P < 0.05$, $^{**}P < 0.01$ (One-way analysis of variance (ANOVA) with Tukey's multiple comparisons test). CPP, cell penetrating peptide; MPLA, Monophosphoryl Lipid A; OVA, ovalbumin.

striking contrast, Z14 was able to induce significant levels of TAA-specific CD8 T cells, when injected with Hiltonol or MPLA.

The therapeutic effect of different combinations of ZEBRA CPP constructs on growth of melanoma lung metastases was then assessed. To establish tumors, mice were injected i.v. with 1×10^5 B16 cells expressing gp100 and OVA antigens. Vaccinations were made with ZEBRA CPP variant vaccines expressing $gp100_{25-33}$ CD8 epitope and the OVA323–339 CD4 epitope (**Figure 8c**). Z14 CPP was the most efficacious variant, supporting previous immune response data (**Figure 8a**). However, an impressive reduction of melanoma lung metastasis was also observed in mice vaccinated with Z13 combined to TAA tyrosinase related protein 2 ($Trp2_{180-188}$), suggesting that combination with Z13 could still be efficacious depending on the antigen (see **Supplementary Figure S5**).

DISCUSSION

Evidence is increasing that CPPs are able to induce potent immune responses via enhanced delivery and presentation. This was first reported in a study using the minimal domain of TAT with OVA protein. TATOVA allows the processing and presentation of both MHC class I and class II, allowing for the generation of both CD8 and CD4 T response.[25] We previously showed that a fusion protein combining ZEBRA CPP with epitope peptides was able to promote CD8 and CD4 T cell responses and antitumor control.[10] In this report, we identified the most efficacious CPP truncations–adjuvants combinations to elicit simultaneous CD8 and CD4 T cell immune responses for both model- and TAA-antigens.

We observed that structural characteristics associated with CPP function (such as alpha-helicity and theoretical pI) varied according to the CPP truncation and cargo epitope composition. Physicochemical properties of the ZEBRA CPP construct were predictive for the *in vitro* efficacy except for *in vitro* CD8 T cell proliferation. The later assay did not allow discrimination between the various truncations conjugated to OVACD8, likely due to the extreme sensitivity of OT-I cells to proliferation stimuli. In striking contrast, CPP variants with theoretical structure properties predicted to be efficacious for cell permeation (*e.g.*, high pI) were associated with high *in vitro* transduction efficiency and stimulation of potent human T cell stimulation (**Figures 3–5**). This was validated by positive correlations between the pI of CPP variants and *in vitro* transduction or human T cell stimulation data (**Supplementary Figure S2**).

Z18 CPP has a low pI and showed the lowest efficacy *in vitro* for both transduction and promotion of MHC class I and II epitope presentation. However, Z18 was shown to elicit potent *in vivo* OVA-specific CD8 and CD4 T cell immune responses (**Figures 6–8**). We hypothesize that this observation may be correlated to a chemical effect due to the formulation (adjuvant/construct). Indeed, it is likely that the mixture of Z18OVACD8CD4 with either the lipopeptide Pam3CSK4 or the monophosphoryl lipid MPLA, formed a temporarily amphiphilic complex, with enhanced translocation and internalization capacity.[26] This adjuvant-ZEBRA CPP complex would thereby allow efficient cargo transport and loading into DCs as well as the simultaneous activation of DCs. In contrast, Z15 showed limited *in vivo* efficacy (**Figures 6** and **7**) compared with the high *in vitro* stimulatory capacities (**Figures 3** and **5**). Indeed, injected without antiCD40 antibody, this construct did not elicit potent CD8 T cell immune response. This low CD8 T cell response was associated with a weak CD4 T cell response when injected with MPLA or Pam3CSK4 (**Figures 7** and **8**). Thus, without any antiCD40 agonist, substituting for the function of CD4 T helper cells,[22] Z15 CPP truncation was not very efficacious for eliciting CTL immune responses. However, this variant vaccine was able to promote high CD4 T cell immune responses when combined with Hiltonol, described

as a powerful adjuvant for T helper responses.[23,24] Further, *in vivo* studies would be therefore necessary to determine whether the low level of CD8 T cell immune responses induced by Z15 CPP was due to inefficient escape from the endosome to the cytosol.[27] Altogether, the results point out that the level of efficacy of a CPP-based vaccine cannot be uniquely related to its *in vitro* capacities.

Whereas Z18 is a potent ZEBRA CPP truncation when conjugated to CD4 and CD8 epitopes of OVA, it was less potent to elicit gp100-specific CD8 T cells when conjugated to this epitope and the OVA CD4 epitope (**Figure 8a,b**). This highlights the importance of the cargo conjugated to the CPP, which may result in: (i) the loss of CPP capacities; (ii) an inefficient escape from the endosome to the cytosol; and (iii) a poor solubility once in a buffered solution. In contrast to Z18, we have demonstrated that Z13 and Z14 were able to elicit TAA-specific CD8 T cell responses. Previous reports showed the capacity of CPP to induce TAA-specific CD8 T cell immune responses using DCs transduced with TAT-Trp2[28] or TAT-carcinoembryonic antigen fusion protein (TAT-CEA) injected with CpG oligodeoxynucleotides or Poly(I:C) as adjuvant.[29,30] Vaccination with penetratin CPP conjugated to mucin 1 (MUC1) epitopes also showed tumor-specific immune responses elicited by CPP.[31] All these data are encouraging for the promotion of TAA-specific immune responses by CPP vectors.

All ZEBRA CPP variants conjugated to CD8 and CD4 epitopes of OVA gave higher immune responses than the cargo alone without CPP. Now, we have evidence that multiepitope cargos can be efficacious, at least, for the OVA and gp100 epitopes tested. These encouraging results will be investigated further to determine whether general rules can be established and extended to other antigen combinations. Our data reveal that adjuvant choice could not be reduced to a single "optimal" combination. Final choice of CPP-based vaccine and adjuvant clearly depends on many factors, but the global measure of antitumor efficacy in an aggressive tumor model remains an essential parameter. In EG7 thymoma bearing mouse experiments, major differences were observed in therapeutic efficacy. Certain adjuvant combinations were identified as having significant *in vivo* impact for all of the CPPs, by either controlling tumor growth (tumor volume or metastasis tumor growth) at early time points, or in prolonging overall survival.

Overall, the results of this study provide valuable information about the potency of the ZEBRA CPP-based vaccines, which is remarkably high in eliciting T cell-mediated immunity and in controlling tumor growth even in aggressive tumor models. We established that to profit from the full potential of ZEBRA CPP variants, choice of adjuvant is the most critical parameter. It was noteworthy that the hierarchy of ZEBRA CPP variants therapeutic effect varied according to the adjuvant used, and according to the strength of the response in the CD4 and the CD8 compartments. Optimal pairing of a particular ZEBRA-CPP sequence and peptide epitope cargo together with a TLR agonist based adjuvant induced well tolerated but potent antitumor immunity. Our results highlight the unique role of *in vivo* testing of novel vaccine constructs together with adjuvants to select combinations for further clinical development. Moreover, future new developments in adjuvants may allow even higher potency to be attained with CPP-based vaccines.

MATERIALS AND METHODS

Cell lines. The EL-4 thymoma cell line was maintained in Roswell Park Memorial Institute medium (RPMI) 1,640 medium supplemented with 10% heat-inactivated fetal calf serum, 10 mmol/l HEPES (*N*-2-hydroxyethylpiperazine-*N9*-*2*-ethanesufonic acid), 100 U/ml penicillin, and 100 U/ml streptomycin (all from Life Technologies, Waltham, MA). The EG.7-OVA cell line (EG7, CRL-2113; American Type Culture Collection), a stable transfectant of the murine OVA-expressing EL-4 thymoma (H-2^b), was maintained in complete RPMI 1,640 medium with 0.5 mg/ml G418 (Life Technologies). The B16-OVA cell line, an OVA-transfected clone derived from the murine melanoma cell line B16 was maintained in complete RPMI 1,640 medium with 1 mg/ml G418 (Life Technologies). The K562 cell line was maintained in Iscove's modified Dulbecco's medium (IMDM, Life Technologies) supplemented with 10% heat-inactivated fetal calf serum, 10 mmol/l HEPES, 100 U/ml penicillin and 100 U/ml streptomycin (all from Life Technologies).

Mice. Female C57BL/6J mice were purchased from Charles River Laboratories. TCR transgenic mice were all on a C57BL/6 background. OTI and OTII mice express TCR specific for OVA epitopes (OTI: MHC class I restricted $OVA_{257–264}$; OTII: MHC class II restricted $OVA_{323–339}$) and were purchased from Charles River (l'Arbresle, France). All animals used in this study were between 6 and 12 weeks of age at the time of experiments. These studies have been reviewed and approved by the institutional and cantonal veterinary authorities in accordance with Swiss Federal law on animal protection.

Cell preparation. Bone marrow derived DCs (BMDCs) were prepared from C57BL/6 mice as previously described,[32] and used at day 9–10 of culture. Human monocyte-derived DCs (mo-DCs) were prepared from Buffy-coats as previously described.[33] Peripheral blood and spleen mononuclear cell suspensions from mice were isolated using Ficoll-Paque gradient (GE Healthcare, Little Chalfont, UK) before flow cytometry analysis or enzyme-linked immunospot (ELISPOT) assay.

Peptide synthesis and CD spectroscopy. Peptides were synthesized on an ABI 433 synthesizer customized to perform Boc chemistry with *in situ* neutralization as already described.[34] Purity and integrity of each peptide were routinely verified by high-performance liquid chromatography and mass spectrometry. CD experiments were carried out in a 0.1 cm quartz cell using a Jasco J-710 spectrometer (Jasco, Easton, MD) with 100 µmol/l peptide solutions (1.25% trifluoroethanol in dH_20) at 20°C.

Proliferation tests. BMDCs were used at day 9–10 of culture as antigen-presenting cells for proliferation tests. Briefly, BMDCs were loaded with 0.3 µmol/l of the indicated peptide for 4 hours at 37°C, washed three times, then matured overnight at 37°C with 100 ng/ml LPS (from *Salmonella abortus*, equi S-form, Enzo Life Sciences, Farmingdale, NY). Antigen-loaded mature BMDC were then mixed at a ratio of 1:10 with the indicated TCR transgenic mouse splenocytes that had been stained with 10 µmol/l 5-(and 6) Carboxyfluorescein diacetate succinimidyl ester (CFSE) (Life Technologies). After 4 days coincubation of spleen cells and BMDCs, antigen-specific proliferation was assessed by flow cytometry, measuring CFSE dilution on live-gated CD8 or CD4 T cells.

Antibodies and flow cytometry. For surface staining, after FcR blocking, the following mAb were used: CD4 (RMA4-4), CD8 (53–6.7), CD11b (M1/70), CD19 (6D5), CD62L (Mel-14), KLRG1 (2F1/KLRG1), all from BD Biosciences (Franklin Lakes, NJ). Dead cells were identified with LIVE/DEAD yellow fluorescent reactive dye (L34959) from Life Technologies and were excluded from analyses. MHC-peptide multimers were from Proimmune (Oxford, UK) or from Immudex (Copenhagen, Denmark). Multimer gating strategy used a dump gate (CD4, CD11b, and CD19) and excluded dead cells. Intracellular cytokines were stained after restimulation with the indicated peptides for 6

hours in the presence of Brefeldin A (GolgiPlug, BD Bioscences) with mAb to IFN-γ (XMG1.2), TNF (MP6-XT22) and corresponding isotype controls (BD Biosciences). Fixation and permeabilization was carried out using BD Bioscience kit according to manufacturer's instructions. For staining of human T cells stimulated with DCs, the following antibodies were used after FcR blocking: CD4 (RPAT4), CD8 (RPAT8), CD107a (H4A3) (BD Biosciences), IFN-γ (4S.B3) and TNF-α (MAb11) (BD Biosciences), all from eBioscience (San Diego, CA), except where noted. Fixation and permeabilization was performed using the PerFix kit from Beckman Coulter according to manufacturer's instructions. Cells were analysed using a Gallios flow cytometer (Beckman Coulter, Brea, CA) or an LSR II flow cytometer (BD Biosciences) and results were processed with FlowJo (FlowJo LLC, Ashland, OR) or Kaluza (Beckman Coulter) software.

ELISPOT assay. The ELISPOT assay for detection of peptide-specific IFN-γ-secreting T cells was performed essentially as described previously.[35] For analysis of *ex vivo* cytokine secretion, splenocytes were incubated overnight in ELISPOT plates in the presence or absence of 5 µmol/l of $OVA_{257-264}$ (OVACD8) or $OVA_{323-339}$ (OVACD4). The number of peptide-specific IFN-γ-producing cells was calculated by subtracting the number of IFN-γ-secreting cells cultured without peptide to that obtained with cells cultured with peptide.

In vitro *transduction assay.* Fluorescein amidite (FAM)-conjugated synthetic ZEBRA CPP truncation constructs were synthesized in-house. Transduction of either BMDC, mo-DCs, EL-4 or K562 cells was carried out at 37°C for 4 hours. For removal of membrane bound peptide prior to cell transduction, an acid wash (0.2 mol/l Glycine, 0.15 mol/l NaCl pH 3.0) was performed. Cells were then analyzed by flow cytometry.

In vitro *epitope presentation (MHC I) assay by human DCs.* DCs from an HLA-$A2^+$ donor were prepared from elutriated monocytes, cultured in CellGro DC medium (CellGenix, Freiburg, Germany) with granulocyte–macrophage colony-stimulating factor (GM–CSF; 2,500 U/ml) (Leucomax; Schering-Plough, Kenilworth, NJ) and IL-4; 1,000 U/ml (CellGenix). The immature DCs were matured with cytokines: IL-1β (10 ng/ml), IL-6 (1,000 U/ml), TNFα; 10 ng/ml (all from CellGenix) and prostaglandin E_2 (1 µg/ml) (Sigma-Aldrich, Saint-Louis, MO). DCs were rested in CellGro DC medium for 2 hours and loaded with 1 µmol/l of Scramble-MART1, Z13-MART1, Z14-MART1, Z15-MART-1, and Z18-MART1 for 4 hours at 37°C before being washed once and plated at 300,000 cells per well in round-bottomed 96-well plates. In addition, nonloaded DCs and DCs loaded with the high affinity MART-1 peptide (ELAGIGILTV) at 1 µmol/l (ProImmune, Oxford, UK) were used as negative and positive controls, respectively.

T cells were expanded from peripheral blood mononuclear cells as previously described[36] using Dynabeads ClinExVivo CD3/CD28 (Life Technologies). Expanded T cells (day 10 postactivation) were transfected with the DMF5 TCR (a kind gift of Dr R. Morgan, National Cancer Institute, Bethesda). This was done either by mRNA electroporation or retroviral transduction as previously described.[36,37] T cells were coincubated with DCs at a ratio of 1:2 for 5 hours in the presence of GolgiPlug and GolgiStop (both BD Biosciences) before intracellular staining was performed as described earlier. All conditions were tested in duplicate, and the experiment was repeated 2–3 times.

Vaccinations. Vaccines were prepared in phosphate-buffered saline (PBS), with 10 nmoles of peptide injected s.c., with the addition of 100 µg anti-CD40 (FGK4.5, Bioxcell, Brandford, CT) when indicated. Hiltonol (50 µg, Poly-ICLC, Oncovir, Washington, DC) was administered i.m., close to the peptide injection site. MPLA (20 µg, Avanti Polar Lipids) was s.c. coinjected with the peptide. Pam3CSK4 (20 µg, Invivogen) was subcutaneously coinjected with the peptide.

In vivo *tumor experiments.* C57BL/6 mice were implanted s.c. with 3×10^5 EG7-OVA tumor cells in the left flank and vaccinated three times (d5, d13, and d24) by s.c. injection of 10 nmoles of peptides and adjuvant as indicated in the right flank. Tumor size was measured with a caliper. Mice were euthanized when tumor reached a diameter of 13 mm.

C57BL/6 mice were implanted i.v. with 1×10^5 B16-OVA tumor cells and vaccinated twice (d-21 and d-7) by s.c. injection of 10 nmoles of peptides with the addition of 100 µg anti-CD40 (FGK4.5, Bioxcell). Hiltonol (50 µg, Poly-ICLC, Oncovir) was administered i.m., close to the peptide injection site. Control mice group was injected with anti-CD40 and Hiltonol. At day 17 postimplantation, lungs were recovered and metastases counted using microscopy.

Statistical analysis. Statistical analyses were performed using Prism 6.0 software (GraphPad Software, La Jolla, CA) and considered statistically significant if $P < 0.05$.

SUPPLEMENTARY MATERIAL

Figure S1. Design of eight variants (Z13 to Z20) based on truncations of ZEBRA CPP Z12.
Figure S2. Correlation graphs between CPP variant theoretical pI value and in vitro results.
Figure S3. CD8 and CD4 T cell immune responses elicited by vaccination with ZEBRA CPP truncations combined to TLR3 agonist (Hiltonol).
Figure S4. CD8 and CD4 T cell immune responses elicited by vaccination with ZEBRA CPP truncations combined to TLR2 agonist (Pam3CSK4) or TLR4 (MPLA).
Figure S5. Effect of Z13Trp2 on control of melanoma lung metastasis growth.
Table S1. Physicochemical properties of the ZEBRA CPP truncations.
Table S2. Physicochemical properties of the ZEBRA CPP truncations conjugated to OVACD8 cargo.
Table S3. Physicochemical properties of the ZEBRA CPP truncations conjugated to MART1 cargo.
Table S4. Physicochemical properties of the ZEBRA CPP truncations conjugated to OVACD8CD4 cargo.
Table S5. Physicochemical properties of the ZEBRA CPP truncations conjugated to OVACD4gp100CD8 cargo.

ACKNOWLEDGMENTS

Funding was provided by the Commission for Technology and Innovation (M.D. and P.R.W.). M.D., P.-Y.D., and P.R.W. are coinventors on two patents related to Z12. M.D. is shareholder in Amal Therapeutics. We thank P.T. for his technical assistance.

REFERENCES

1. Melero, I, Gaudernack, G, Gerritsen, W, Huber, C, Parmiani, G, Scholl, S *et al.* (2014). Therapeutic vaccines for cancer: an overview of clinical trials. *Nat Rev Clin Oncol* **11**: 509–524.
2. Marusyk, A and Polyak, K (2010). Tumor heterogeneity: causes and consequences. *Biochim Biophys Acta* **1805**: 105–117.
3. Rabinovich, GA, Gabrilovich, D and Sotomayor, EM (2007). Immunosuppressive strategies that are mediated by tumor cells. *Annu Rev Immunol* **25**: 267–296.
4. Wu, AA, Drake, V, Huang, HS, Chiu, S and Zheng, L (2015). Reprogramming the tumor microenvironment: tumor-induced immunosuppressive factors paralyze T cells. *Oncoimmunology* **4**: e1016700.
5. Dunn, GP, Bruce, AT, Ikeda, H, Old, LJ and Schreiber, RD (2002). Cancer immunoediting: from immunosurveillance to tumor escape. *Nat Immunol* **3**: 991–998.
6. Guo, C, Manjili, MH, Subjeck, JR, Sarkar, D, Fisher, PB and Wang, XY (2013). Therapeutic cancer vaccines: past, present, and future. *Adv Cancer Res* **119**: 421–475.
7. van Montfoort, N, Camps, MG, Khan, S, Filippov, DV, Weterings, JJ, Griffith, JM *et al.* (2009). Antigen storage compartments in mature dendritic cells facilitate prolonged cytotoxic T lymphocyte cross-priming capacity. *Proc Natl Acad Sci USA* **106**: 6730–6735.
8. Toes, RE, Offringa, R, Blom, RJ, Melief, CJ and Kast, WM (1996). Peptide vaccination can lead to enhanced tumor growth through specific T-cell tolerance induction. *Proc Natl Acad Sci USA* **93**: 7855–7860.
9. Rosalia, RA, Quakkelaar, ED, Redeker, A, Khan, S, Camps, M, Drijfhout, JW *et al.* (2013). Dendritic cells process synthetic long peptides better than whole protein, improving antigen presentation and T-cell activation. *Eur J Immunol* **43**: 2554–2565.
10. Derouazi, M, Di Berardino-Besson, W, Belnoue, E, Hoepner, S, Walther, R, Benkhoucha, M *et al.* (2015). Novel cell-penetrating peptide-based vaccine induces robust $CD4^+$ and $CD8^+$ T cell-mediated antitumor immunity. *Cancer Res* **75**: 3020–3031.

11. Copolovici, DM, Langel, K, Eriste, E and Langel, Ü (2014). Cell-penetrating peptides: design, synthesis, and applications. *ACS Nano* **8**: 1972–1994.
12. Milletti, F (2012). Cell-penetrating peptides: classes, origin, and current landscape. *Drug Discov Today* **17**: 850–860.
13. Frankel, AD and Pabo, CO (1988). Cellular uptake of the tat protein from human immunodeficiency virus. *Cell* **55**: 1189–1193.
14. Tacken PJ, Joosten B, Reddy A, Wu D, Eek A, Laverman P, et al. (2008). No advantage of cell-penetrating peptides over receptor-specific antibodies in targeting antigen to human dendritic cells for cross-presentation. *J Immunol* **180**: 7687–7696.
15. Joliot, A, Pernelle, C, Deagostini-Bazin, H and Prochiantz, A (1991). Antennapedia homeobox peptide regulates neural morphogenesis. *Proc Natl Acad Sci USA* **88**: 1864–1868.
16. Derossi, D, Joliot, AH, Chassaing, G and Prochiantz, A (1994). The third helix of the Antennapedia homeodomain translocates through biological membranes. *J Biol Chem* **269**: 10444–10450.
17. Deshayes, S, Decaffmeyer, M, Brasseur, R and Thomas, A (2008). Structural polymorphism of two CPP: an important parameter of activity. *Biochim Biophys Acta* **1778**: 1197–1205.
18. Eiríksdóttir, E, Konate, K, Langel, U, Divita, G and Deshayes, S (2010). Secondary structure of cell-penetrating peptides controls membrane interaction and insertion. *Biochim Biophys Acta* **1798**: 1119–1128.
19. Rothe, R, Liguori, L, Villegas-Mendez, A, Marques, B, Grunwald, D, Drouet, E *et al.* (2010). Characterization of the cell-penetrating properties of the Epstein-Barr virus ZEBRA trans-activator. *J Biol Chem* **285**: 20224–20233.
20. Matsumoto, R, Okochi, M, Shimizu, K, Kanie, K, Kato, R and Honda, H (2015). Effects of the properties of short peptides conjugated with cell-penetrating peptides on their internalization into cells. *Sci Rep* **5**: 12884.
21. Greenfield, NJ (1996). Methods to estimate the conformation of proteins and polypeptides from circular dichroism data. *Anal Biochem* **235**: 1–10.
22. Hassan, SB, Sørensen, JF, Olsen, BN and Pedersen, AE (2014). Anti-CD40-mediated cancer immunotherapy: an update of recent and ongoing clinical trials. *Immunopharmacol Immunotoxicol* **36**: 96–104.
23. Trumpfheller, C, Caskey, M, Nchinda, G, Longhi, MP, Mizenina, O, Huang, Y *et al.* (2008). The microbial mimic poly IC induces durable and protective $CD4^+$ T cell immunity together with a dendritic cell targeted vaccine. *Proc Natl Acad Sci USA* **105**: 2574–2579.
24. Longhi, MP, Trumpfheller, C, Idoyaga, J, Caskey, M, Matos, I, Kluger, C *et al.* (2009). Dendritic cells require a systemic type I interferon response to mature and induce $CD4^+$ Th1 immunity with poly IC as adjuvant. *J Exp Med* **206**: 1589–1602.
25. Shibagaki, N and Udey, MC (2002). Dendritic cells transduced with protein antigens induce cytotoxic lymphocytes and elicit antitumor immunity. *J Immunol* **168**: 2393–2401.
26. Di Pisa, M, Chassaing, G and Swiecicki, JM (2015). When cationic cell-penetrating peptides meet hydrocarbons to enhance in-cell cargo delivery. *J Pept Sci* **21**: 356–369.
27. Qian, Z, Dougherty, PG and Pei, D (2015). Monitoring the cytosolic entry of cell-penetrating peptides using a pH-sensitive fluorophore. *Chem Commun (Camb)* **51**: 2162–2165.
28. Shibagaki, N and Udey, MC (2003). Dendritic cells transduced with TAT protein transduction domain-containing tyrosinase-related protein 2 vaccinate against murine melanoma. *Eur J Immunol* **33**: 850–860.
29. Woo, SJ, Kim, CH, Park, MY, Kim, HS, Sohn, HJ, Park, JS *et al.* (2008). Co-administration of carcinoembryonic antigen and HIV TAT fusion protein with CpG-oligodeoxynucleotide induces potent antitumor immunity. *Cancer Sci* **99**: 1034–1039.
30. Park, JS, Kim, HS, Park, HM, Kim, CH and Kim, TG (2011). Efficient induction of anti-tumor immunity by a TAT-CEA fusion protein vaccine with poly(I:C) in a murine colorectal tumor model. *Vaccine* **29**: 8642–8648.
31. Apostolopoulos, V, Pouniotis, DS, van Maanen, PJ, Andriessen, RW, Lodding, J, Xing, PX *et al.* (2006). Delivery of tumor associated antigens to antigen presenting cells using penetratin induces potent immune responses. *Vaccine* **24**: 3191–3202.
32. Santiago-Raber, ML, Baccala, R, Haraldsson, KM, Choubey, D, Stewart, TA, Kono, DH *et al.* (2003). Type-I interferon receptor deficiency reduces lupus-like disease in NZB mice. *J Exp Med* **197**: 777–788.
33. Landmann, S, Mühlethaler-Mottet, A, Bernasconi, L, Suter, T, Waldburger, JM, Masternak, K *et al.* (2001). Maturation of dendritic cells is accompanied by rapid transcriptional silencing of class II transactivator (CIITA) expression. *J Exp Med* **194**: 379–391.
34. Hartley, O, Gaertner, H, Wilken, J, Thompson, D, Fish, R, Ramos, A *et al.* (2004). Medicinal chemistry applied to a synthetic protein: development of highly potent HIV entry inhibitors. *Proc Natl Acad Sci USA* **101**: 16460–16465.
35. Miyahira, Y, Murata, K, Rodriguez, D, Rodriguez, JR, Esteban, M, Rodrigues, MM *et al.* (1995). Quantification of antigen specific $CD8^+$ T cells using an ELISPOT assay. *J Immunol Methods* **181**: 45–54.
36. Almåsbak, H, Rian, E, Hoel, HJ, Pulè, M, Wälchli, S, Kvalheim, G *et al.* (2011). Transiently redirected T cells for adoptive transfer. *Cytotherapy* **13**: 629–640.
37. Wälchli, S, Løset, GÅ, Kumari, S, Johansen, JN, Yang, W, Sandlie, I *et al.* (2011). A practical approach to T-cell receptor cloning and expression. *PLoS One* **6**: e27930.